Published in final edited form as:

Brain Res. 2018 October 15; 1697: 45–52. doi:10.1016/j.brainres.2018.06.013.

Correcting deregulated *Fxyd1* expression rescues deficits in neuronal arborization and potassium homeostasis in MeCP2 deficient male mice

Valerie Matagne[a,*,1], **Joyce Wondolowski**[b], **Matthew Frerking**[c], **Mohammad Shahidullah**[d], **Nicholas A. Delamere**[d], **Ursula S. Sandau**[a,2], **Sarojini Budden**[e], **Sergio R. Ojeda**[a,*]

[a]Division of Neuroscience, Oregon National Primate Research Center/Oregon Health & Science University, Beaverton, OR 97006, USA

[b]Neuroscience Graduate Program, Oregon Health and Sciences University, Portland, OR 97239, USA

[c]Departments of Behavioral Neuroscience, Oregon Health & Science University, Portland, OR 97239, USA

[d]Department of Physiology, University of Arizona, Tucson, AZ 85721, USA

[e]Division of Developmental Pediatrics, Oregon Health & Science University, Portland, OR 97239, USA

Abstract

Rett syndrome (RTT) is a neurodevelopmental disorder caused by mutations in the *MECP2* gene. In the absence of MeCP2, expression of FXYD domain-containing transport regulator 1 (FXYD1) is deregulated in the frontal cortex (FC) of mice and humans. Because Fxyd1 is a membrane protein that controls cell excitability by modulating Na^+, K^+-ATPase activity (NKA), an excess of Fxyd1 may reduce NKA activity and contribute to the neuronal phenotype of *Mecp2* deficient (KO) mice. To determine if Fxyd1 can rescue these RTT deficits, we studied the male progeny of *Fxyd1* null males bred to heterozygous *Mecp2* female mice. Maximal NKA enzymatic activity was not altered by the loss of MeCP2, but it increased in mice lacking one *Fxyd1* allele, suggesting that NKA activity is under Fxyd1 inhibitory control. Deletion of one *Fxyd1* allele also prevented the increased extracellular potassium (K^+) accumulation observed in cerebro-cortical neurons from *Mecp2* KO animals in response to the NKA inhibitor ouabain, and rescued the loss

*Corresponding authors at: Human Neurogenetics, Aix Marseille Univ, INSERM, MMG, U1251, Marseille, France; 27 bd Jean Moulin, 13385 Marseille Cedex 5, France (Valerie Matagne, Valerie.matagne@univ-amu.fr). Division of Neuroscience, Oregon National Primate Research Center, 505 NW 185th Ave, Beaverton, OR 97006, USA (Sergio R. Ojeda, ojedas@ohsu.edu).

5. Contributors

All authors had full access to all the data in the study and take responsibility for the integrity of the data and the accuracy of the data analysis. Study concept and design: SRO, VM. Acquisition of data: VM, JW, MF, MS, NAD, USS, SRO. Analysis and interpretation of data: VM, MF, MS, NAD, SRO. Drafting the manuscript: VM, SRO. Critical revision of the manuscript for important intellectual content: VM, NAD, MS, MF, SRO, SB. Statistical analysis: VM, MF, SRO, MS. Obtained funding: VM, MF, NAD, SRO. Study supervision: SRO.

[1]Present address for VM: Aix Marseille Univ, INSERM, MMG, U1251, Marseille, France, 27 bd Jean Moulin, 13385, Marseille Cedex 5, France.

[2]Present address for USS: Oregon Health & Science University, 3181 SW Sam Jackson Park Rd Portland, OR 97239.

6. Conflict of interest

The authors have nothing to declare.

of dendritic arborization observed in FC neurons of *Mecp2* KO mice. These effects were gene-dose dependent, because the absence of Fxyd1 failed to rescue the MeCP2-dependent deficits, and mimicked the effect of MeCP2 deficiency in wild-type animals. These results indicate that excess of Fxyd1 in the absence of MeCP2 results in deregulation of endogenous K^+ conductances functionally associated with NKA and leads to stunted neuronal growth.

Keywords

Mecp2 deficiency; Neuronal morphology; Potassium efflux; Sodium-potassium ATPase; Rett syndrome

1. Introduction

Rett syndrome (RTT) is a severe neurodevelopmental disorder (Bienvenu et al., 2000; Bienvenu and Chelly, 2006; Chahrour and Zoghbi, 2007; Wan et al., 1999) primarily caused by inactivating mutations of the nuclear protein methyl-CpG binding protein 2 (*MECP2*) (Amir et al., 1999; Bienvenu et al., 2000; Wan et al., 1999).

Because most of the neurological abnormalities observed in RTT are recapitulated by genetic deletion of the *Mecp2* gene in mice (Chen et al., 2001; Guy et al., 2001; Kishi and Macklis, 2004), these animals have been extensively used to gain insights into the neuropathology of RTT. It is now clear that despite its global effect on changes in neuronal chromatin structure (Skene et al., 2010), a significant fraction of MeCP2 control on gene expression is exerted in a region-dependent manner (Belichenko et al., 1997; Kishi and Macklis, 2005; Shahbazian et al., 2002a). By inference, it would be expected that MeCP2 deficiency might also disrupt specific cellular functions in a region-dependent manner. This outcome is conspicuous in the case of decreased neuronal arborization and reduced numbers of dendritic spines, the two most salient neuromorphological phenotypes of RTT (Armstrong et al., 1995; Armstrong et al., 1998; Belichenko et al., 1997; Belichenko and Dahlstrom, 1995). Both deficits are for the most part restricted to selected subregions of the frontal (FC) and motor cortex (Armstrong et al., 1995; Armstrong et al., 1998; Belichenko et al., 1997; Belichenko and Dahlstrom, 1995), despite the abundance of MeCP2 throughout the brain and spinal cord (Mullaney et al., 2004; Shahbazian et al., 2002a; Tudor et al., 2002).

We and others have previously shown that *FXYD1*, a gene encoding phospholemman (PLM, FXYD1), a membrane protein that modulates Na^+, K^+-ATPase (NKA) activity (Crambert et al., 2002; Feschenko et al., 2003) is an MeCP2 target gene (Deng et al., 2007; Jordan et al., 2007). We also observed that FXYD1 expression is regulated by MeCP2 in a region-dependent manner in both humans and mice (Deng et al., 2007), with Fxyd1 expression increasing in the frontal cortex (FC), but not the cerebellum (CB) of *Mecp2* KO mice (Deng et al., 2007) and mutant mice carrying a truncated form of MeCP2 (Matagne et al., 2013).

FXYD1 has been shown to maintain neuronal excitability (Garcia-Rudaz et al., 2008), and to be a major substrate for several kinases, including protein kinase A (PKA), protein kinase C (PKC), myotonic dystrophy protein kinase (DMPK), and never in mitosis (NIMA) kinase (Mounsey et al., 1999; Mounsey et al., 2000; Palmer et al., 1991; Presti et al., 1985; Walaas

et al., 1988; Walaas et al., 1994). These observations suggest that, in addition to modulating NKA activity (Feschenko et al., 2003), Fxyd1 may serve as a nodal point for integration of cell signaling events initiated by the activation of multiple kinases.

In the present study, we bred *Fxyd1* null mice (Jia et al., 2005) to heterozygote female mice lacking one *Mecp2* allele (Guy et al., 2001), and conducted experiments to determine if partial and/or total loss of *Fxyd1* expression can rescue the reduced neuronal arborization of FC neurons observed in *Mecp2* KO mice (Armstrong et al., 1995; Armstrong et al., 1998; Belichenko et al., 1997; Belichenko and Dahlstrom, 1995). Because FXYD1 is a regulator of NKA activity (Crambert and Geering, 2003), and the electrophysiological response to NKA inhibition is altered in FC neurons of *Mecp2* null mice (Deng et al., 2007), we also sought to determine if NKA enzymatic activity was altered in the FC of *Mecp2* null mice, and if these alterations could be reversed by reducing or abolishing *Fxyd1* expression.

2. Results

2.1. Changes in MeCP2 and Fxyd1 content in the FC of Mecp2 and Fxyd1-deficient mice

To determine if the animals subjected to genetic ablation of *Mecp2* and *Fxyd1* alleles exhibited the expected genotype-dependent changes in MeCP2 and Fxyd1 content in the FC, we measured by Western blot the abundance of both MeCP2 and FXYD1 in the FC of mutant mice. As expected, MeCP2 was detected only in the *Mecp2* WT group (Fig. 1A). In agreement with earlier observations (Deng et al., 2007), the abundance of Fxyd1 increased approximately 2-fold in the absence of MeCP2 (Fig. 1B). It decreased by about 50% in animals with one deleted *Fxyd1* allele, and was undetectable in *Fxyd1* KOs (Fig. 1C).

2.2. Deletion of one Fxyd1 allele rescues the deficient neuronal dendritic arborization observed in Mecp2 null mice

Golgi staining was used to identify pyramidal neurons in the FC of 7-week-old mice. In agreement with earlier findings (Belichenko et al., 2009; Fukuda et al., 2005), the length and complexity of the dendritic tree of pyramidal neurons was significantly reduced ($p < 0.05$, $F > 3.364$ for soma distances of 50 to 170 μm) in *Mecp2* null mice (*Mecp2* KO/*Fxyd1* WT) as compared to WT controls (*Mecp2* WT/*Fxyd1* WT) (Fig. 2A). Deletion of one *Fxyd1* allele almost completely rescued this defect as the *Mecp2* KO/*Fxyd1* HT group exhibited neurite lengths that were similar to those detected in the *Mecp2* WT/*Fxyd1* WT group for soma distances between 50 and 150 μm (Fig. 2A). The only distances shorter than in WT controls ($p < 0.05$, $F > 3.999$) were those ranging from 160 to 170 μm (Fig. 2A). This rescue effect is gene-dose dependent, because deletion of both *Fxyd1* alleles on either *Mecp2* KO mice (Fig. 2A) or in *Mecp2* WT mice (Fig. 2B) resulted in dendrite lengths indistinguishable from those in *Mecp2* KO mice, ($p < 0.05$, $F > 3.364$ vs. *Mecp2* WT animals for soma distances of 50 to 170 μm). Surprisingly, deletion of one *Fxyd1 allele* in *Mecp2* WT mice also resulted in a loss of dendrite growth similar to those in *Mecp2* KO animals (Fig. 2B). Examples of 3D reconstructions of a WT neuron and *Mecp2* null neurons with either an intact *Fxyd1* gene, or lacking one *Fxyd1* allele are shown in Fig. 2C. From these experiments, we conclude that the defect in dendrite length seen in neurons from *Mecp2* KO mice is rescued by the loss of one *Fxyd1* allele through a *bona-fide* interaction between the two genes.

2.3. Loss of one Fxyd1 allele increases NKA enzymatic activity in the FC of Mecp2 null mice

We previously found (Deng et al., 2007) that FC neurons express a ouabain-induced inward current that is reduced in *Mecp2* KO mice, suggesting that NKA activity is impaired in these neurons. To more directly assess this possibility, we measured maximal NKA activity in the FC and three other brain regions (occipital cortex, hippocampus and cerebellum) utilizing a biochemical assay that determines ouabain-sensitive ATP hydrolysis under Vmax conditions (Tamiya et al., 2007). Although no detectable change in maximal NKA activity was observed in the FC of *Mecp2* KO mice compared to WT animals (Fig. 3), deletion of one *Fxyd1* allele resulted in a significant increase in ouabain-sensitive activity in both *Mecp2* WT and *Mecp2* KO mice (Fig. 3), indicating that – as shown by others (Crambert et al., 2002; Feschenko et al., 2003) – Fxyd1 has a repressive effect on NKA activity. This increase seemed to be region-specific since there was no significant alteration in ouabain-sensitive NKA activity in the other brain regions studied (not shown).

2.4. Accumulation of extracellular K^+ following blockade of NKA with ouabain, is increased in Mecp2 KO mice, and this defect is rescued by deletion of one Fxyd1 allele

If maximal NKA activity is unaffected in *Mecp2* KO mice, why does ouabain induce a smaller inward current in FC neurons from these animals? To directly assess the effect of ouabain on specific ion fluxes across the cell membrane, we recorded extracellular K^+ concentration in acute FC slices using K^+-selective microelectrodes. To our surprise, we found that the application of 100 μM ouabain led to a faster build-up of extracellular K^+ in slices from the *Mecp2* KO mice relative to their WT counterparts (Fig. 4).

To determine whether the enhanced K^+ accumulation seen in *Mecp2* KO mice was related to increased Fxyd1 expression, we examined whether the accumulation was reversed in *Mecp2* KO mice lacking one *Fxyd1* allele (*Mecp2* KO/*Fxyd1* HT) (Fig. 4). We found that this was indeed the case, with a significantly slower rise in K^+ in the double mutant mice that was similar to the one seen in WT mice. In *Mecp2* WT/*Fxyd1* HT mice, ouabain led to essentially no accumulation of K^+, suggesting that the steady-state K^+ turnover is very low in tissue from these mice. We did not examine the effect of deleting both *Fxyd1* alleles on extracellular K^+ accumulation of *Mecp2* KO mice, because total NKA activity was not affected in these animals Collectively, these results suggest that outwardly directed leakage of cellular K^+ induced by ouabain is enhanced by genetic ablation of *Mecp2* and that reduction of *Fxyd1* expression rescues this phenotype, in keeping with the finding that loss of one *Fxyd1* allele leads to increased NKA biochemical activity.

3. Discussion

FXYD1 is a gene that becomes deregulated in the absence of MECP2 in the FC of both humans affected by RTT and male *Mecp2* KO mice (Deng et al., 2007). An increased *Fxyd1* expression is brain region-specific as is detected in the FC, but not the CB, of *Mecp2*-deficient mice and appears to be the direct consequence of a loss of MeCP2-dependent transcriptional repression (Banine et al., 2011; Deng et al., 2007).

In the present study, we employed *Mecp2* KO mice (Guy et al., 2001; Shahbazian et al., 2002b) to carry out studies aimed at determining if correcting *Fxyd1* overexpression was able to rescue or ameliorate some of the neuronal impairments affecting these animals. We observed that deletion of one *Fxyd1* allele, which brings Fxyd1 protein levels back down to WT values, rescues the stunted dendritic arborization characteristically seen in cerebro-cortical neurons of animals lacking MeCP2 (Belichenko et al., 2008; Belichenko et al., 2009; Fukuda et al., 2005). These findings are consistent with a previous study (Deng et al., 2007) showing that overexpressing Fxyd1 in cultured FC neurons at levels identical to those observed in the FC of *Mecp2* KO mice, results in reduced dendritic arborization and spine formation.

The overall importance of Fxyd1 in the regulation of basic brain functions has been evidenced by reports showing that: a) Fxyd1 is required for the formation of the ventricular system (Chang et al., 2012), b) in the absence of RNG105, an RNA binding protein, there is reduced dendritic localization of the mRNAs for NKA, Fxyd1, Fxyd6 and Fxyd7, causing loss of dendritic development and an altered pattern of synaptic protein distribution in the mouse cerebral cortex (Shiina et al., 2010), and c) the specific loss of Fxyd1, via RNAi, results in decreased attachment of synapsin I to spines, suggesting that Fxyd1 promotes the attachment of excitatory presynapses to spines (Shiina et al., 2010). In line with these observations, Fxyd1 has been shown to play a role in maintaining neuronal excitability to incoming transsynaptic stimulatory inputs (Garcia-Rudaz et al., 2008).

Given the many roles of MeCP2, it is not surprising that the dendritic loss seen in its absence results from the interplay of different mechanisms, such as defects in astrocytic function (Ballas et al., 2009), lack of MeCP2 phosphorylation (Zhou et al., 2006), and miRNA deregulation (Zhang et al., 2016). We reasoned that NKA might also be involved, because Fxyd1 represses NKA activity (Crambert et al., 2002; Crambert and Geering, 2003), and Fxyd1 expression increases in the absence of MeCP2. NKA is responsible for maintaining Na^+ and K^+ gradients across the cell membrane (Lees, 1991), thereby playing a critical role in restoring the electro-chemical gradient of Na^+ and K^+ ions after neuronal excitation (Lees, 1991). A substantial body of evidence now exists showing that NKA activity in mammalian tissues is regulated by FXYD family members (see for instance (Bossuyt et al., 2009; Feschenko et al., 2003; Jia et al., 2005; Zhang et al., 2006)). Although Fxyd7 appears to be a brain-specific regulator of NKA activity (Béguin et al., 2002), *Fxyd1*, and not *Fxyd7*, expression is deregulated in the FC of RTT patients and *Mecp2* KO mice (Deng et al., 2007; Jordan et al., 2007).

Contrary to our expectations, maximal NKA biochemical activity was not reduced in *Mecp2* KO mice, an observation at odds with our earlier finding of reduced ouabain-induced currents in FC neurons of *Mecp2* null mice (Deng et al., 2007). However, this apparent discrepancy appears to simply reflect the inability of our biochemical assay to detect small reductions in Na^+, K^+-ATPase activity. The assay measures V_{max} in a homogenate that contains a mixture of neurons, glial and vascular tissue, instead of the steady state activity displayed by neurons under physiological conditions. At steady state, the cellular rate of Na^+-K^+ exchange is considerably less than the V_{max} as only small changes in enzymatic activity are required for maintaining cytoplasmic Na^+/K^+ homeostasis. Although such small

decreases in NKA activity can be reliably measured by detecting reductions in ouabain-dependent inward currents (Deng et al., 2007), they may not be entirely due to loss of NKA activity because the concentration gradients of Na^+ and K^+ are also used to maintain ion gradients for several other ions through passive and active transport mechanisms (e.g., Na^+/Ca^{2+}, Na^+/H^+ and H^+/K^+ exchangers). As a result of this, the transmembrane current induced by ouabain reflects the summed flow of multiple ions, and a change in the total current need not reflect only the electrogenic transport activity of NKA. In line with this interpretation, the present results show an alteration in K^+ homeostasis as blockade of the NKA pump with ouabain resulted in a much greater accumulation of extracellular K^+ in the FC of *Mecp2* null mice than in WT controls.

This exaggerated K^+ response might be due to hyper-activation of a K^+ conductance(s) that is secondary to inactivation of the NKA pump. Because NKA is associated with an A-type K^+ current that interacts with other K^+ conductances to modulate neuronal activity (Glanzman, 2010; Pulver and Griffith, 2010), the possibility exists that an excess of Fxyd1 in the absence of MeCP2 may be activating one or more of these voltage-gated K^+ currents. It is also possible that the capacity of astrocytes to uptake extracellular K^+ via Ca^{2+} dependent-mediated mechanisms (Wang et al., 2012) is reduced in in the absence of MeCP2. This would be consistent with the defects in astrocytic function observed in *Mecp2*-deficient animals (Ballas et al., 2009). Because astrocytes of the FC do not express immunohistochemically detectable levels of *Fxyd1* (Deng et al., 2007), an astrocytic site of action would imply the existence of a communication pathway able to convey the status of Fxyd1 from neurons to astrocytes. Future experiments are required to distinguish between these possibilities.

Relevant to these considerations is the finding that deletion of one *Fxyd1* allele not only increased total NKA activity, but – importantly - rescued both the defect in dendritic growth and K+ homeostasis of *Mecp2* KO neurons. While the former effect is in keeping with the concept that Fxyd1 is an inhibitor of NKA activity (Crambert et al., 2002; Crambert and Geering, 2003; Deng et al., 2007), the mechanisms underlying the effect of Fxyd1 on neuronal morphology and K^+ homeostasis remain to be identified. Fxyd1 could exert these effects by regulating intracellular Ca^{2+} levels and/or Ca^{2+}-dependent intracellular pathways through its inhibition of the Na^+/Ca^{2+} exchanger NCX1 (Ahlers et al., 2005; Mirza et al., 2004; Zhang et al., 2003). On the other hand, Fxyd1 could also act through modulation of intracellular signaling pathways (Xie and Askari, 2002). Fxyd1 can be phosphorylated by various protein kinases (PK) including PKA and PKC activated by adrenergic stimulation (Palmer et al., 1991; Walaas et al., 1994), and the myotonic dystrophy protein kinase (Mounsey et al., 2000), indicating that it may be able to integrate signaling events initiated by more than one kinase. In addition, Fxyd1 could indirectly repress intracellular signaling via inhibition of NKA, as NKA activation results in CREB, ERK1/2 and CamK activation (Desfrere et al., 2009).

The rescuing effect of Fxyd1 is gene dose-dependent as is only apparent in the absence of one allele. Loss of both alleles not only failed to reproduce the phenotype of *Fxyd1* HTs, but instead resulted in a neuronal morphology and NKA activity similar to *Mecp2* KO mice. These observations indicate that the *Fxyd1* gene needs to be expressed at the right level to

sustain normal function. This feature of *Fxyd1* biology is of great interest, because of its similarity to MeCP2, which either in excess or abatement, results in neurological phenotypes (Chao and Zoghbi, 2012).

Altogether these observations support the idea that deregulation of Fxyd1 is responsible for the alterations in ion homeostasis and dendrite development caused by the absence of MeCP2. Although MeCP2 deficiency causes a devastating disease, it appears that this condition is reversible in mice (Guy et al., 2007; Robinson et al., 2012). However, achieving a correct *MECP2* dosage remains a significant obstacle to the use of MECP2 as a target in drug-mediated therapeutic intervention (Chao and Zoghbi, 2012). An alternative approach is the regulation of MECP2 targets, as observed when manipulating BDNF and IGF1 level in mouse models (Chang et al., 2006; Tropea et al., 2009). We recently showed that preventing the increase in Fxyd1 expression that occur in mice carrying a truncated form of the *Mecp2* gene rescues a behavioral impairment in these animals (Matagne et al., 2013). Adding to these results, we show here that manipulating *Fxyd1* expression rescues two different impairments in *Mecp2*-deficient mice: the stunted development of FC neurons, and the exaggerated accumulation of extracellular K^+ in response to blockade of NKA activity. Because Fxyd1 is a protein localized to the cell membrane, it should be readily accessed by small molecules designed to modify its function, and thus provide an additional tool for therapeutic intervention in RTT.

4. Experimental procedures

4.1. Animals

The animals were housed in ONPRC rodent facilities under a 12:12 h light/dark cycle (lights on at 0700) and given *ad libitum* access to food and water. All experiments were conducted in accordance with NIH guidelines and approved by the Institutional Animal Care and Use Committee of OHSU.

The *Mecp2*-deficient (KO) mice (B6,129P2(C)-*Mecp2* tm1-1Bird) were purchased from the Jackson Laboratory (Jackson laboratories, Sacramento, CA) and the *Fxd1*- deficient mice were obtained from Dr A.L Tucker (Division of Cardiovascular Medicine, University of Virginia Health System, Charlottesville, VA, USA). Both lines were maintained on a C57BL/6 background. Genotyping was performed as previously described (Jia et al., 2005; Miralves et al., 2007; Shahbazian et al., 2002b).

Heterozygous *Mecp2* female mice were bred to homozygous male mice lacking the *Fxyd1* gene (Jia et al., 2005). The F1 offspring resulting from these crosses was backcrossed for over five generations onto the C57BL6/J background. The F1 female mice were wild-type (WT) or heterozygous (HT) for the *Mecp2* deletion, and heterozygous for the *Fxyd1* deletion. The F1 male mice were WT or hemizygous for the *Mecp2* mutation and HT for the *Fxyd1* deletion. By crossing F1 mice, six possible genotypes were generated (see below). They were: (i) *Mecp2* WT/*Fxyd1* WT, (ii) *Mecp2* WT/*Fxyd1* HT, (iii) *Mecp2* WT/*Fxyd1* KO, (iv) *Mecp2* KO/*Fxyd1* WT, (v) *Mecp2* KO/*Fxyd1* HT and (vi) *Mecp2* KO/*Fxyd1* KO.

4.2. Protein extraction and Western blotting

Seven-week-old males were sacrificed by cervical dislocation and different brain areas were bilaterally dissected. Proteins were extracted from FC samples in 400 µl of freshly prepared RIPA lysis buffer (10 mM Tris, pH 7.4, 0.1% SDS, 0.5% Deoxicholic acid, 1% Triton X-100, NaCl 150 mM, 80 uM aprotinin, 2 uM Leupeptin, 1.5 uM Pepstatin and 1 mM PMSF). The protein content was measured using the Pierce 660 nm Protein Assay. Two and an half µg of protein were loaded on a precasted 14% Tris-glycine gel (Thermo Fisher Scientific) under denaturing conditions (3% β-mercaptoethanol) and transferred to an Immobilon-P membrane (Millipore, Billerica, MA) using a gel transfer device (Idea Scientific Co., Minneapolis, MN) at 100 mAmp/ 23 V for 2 h at 4 °C. The membrane was blocked with 5% nonfat milk-TBST (Tris buffer saline with 0.05% Tween 20) and incubated overnight at 4 °C with FXYD1 and GAPDH antibodies diluted 1:1000 and 1:20,000, respectively. The next day, the membranes were washed (five changes of TBST every 10 min), before incubating them for 1 h at room temperature with both goat anti-rabbit and goat anti-mouse antibodies conjugated to HRP (both from Zymed Laboratories, San Francisco, CA) each diluted 1:25,000 in TBST buffer. After five more washes with TBST buffer, immunoreactivity was visualized using Pierce ECL or West Dura reagents (Thermo Fisher Scientific, Rockford, IL) and UltraCruz autoradiography Blue films (Santa Cruz Biotechnology, Santa Cruz, CA). The membrane was then incubated overnight at 4 °C with MECP2 antibodies (1:2,000) followed by 1 h incubation with goat anti-rabbit antibody conjugated to HRP (1:25,000), and the immunoreaction was visualized as described above. Densitometric analysis was performed using AlphaEaseFC software (Alpha Innotech, Santa Clara, CA), and the values obtained were normalized for procedural losses using GAPDH as the reference.

4.3. Measurement of NKA activity

Seven-week-old males were sacrificed by cervical dislocation and tissue samples from the frontal cortex (FC), cerebellum (CB), occipital cortex (oCTX) and hippocampus (HC) were bilaterally dissected, frozen in liquid nitrogen and stored at −80 °C until assay. Samples were homogenized in 400 µl of an ice-cold double-strength ATPase assay buffer that contained (mM): L-Histidine, 80; NaCl 200; KCl, 10; $MgCl_2$, 6.0; EGTA, 2.0 (pH 7.4) and one tablet containing a complete protease inhibitor cocktail (Roche Applied Science, Mannheim, Germany) for each 7 ml of ATPase buffer. To avoid overheating, the homogenization protocol was 4 cycles of 15 sec at 5 sec intervals using a Misonix S3000 sonicator at 6 W power setting (Misonix, New York, USA). The homogenate was centrifuged at 13,000g for 30 min at 4 °C to remove nuclei and unbroken cell debris. The pellet was discarded and the supernatant was diluted to a total volume of 1 ml by adding 600 µl of the same ice-cold double-strength ATPase assay buffer containing a protease inhibitor cocktail (see above). The supernatant was then subjected to ultracentrifugation at 140,000×*g* for 1 h at 4 °C (Beckman Rotor 50 Ti, 42,000 rpm). The supernatant was discarded and the pellet, which represents the crude membrane fraction, was suspended in 200 µl of the double-strength ATPase assay buffer and briefly sonicated for 15 sec using the Misonix S3000 sonicator at the 3 W power setting. Protein was measured in the crude membrane preparation by the bicinchoninic acid (BCA) assay (Smith et al., 1985) (Pierce Biotechnology, Rockford, IL, USA), using bovine serum albumin as a standard. The crude

membrane preparation was used to measure NKA activity using a modification of the protocol described earlier (Shahidullah et al., 2012). NKA activity was measured by placing samples of each membrane preparation (approx 50 μg protein) in duplicate tubes to which double-strength ice-cold NKA buffer was added to bring the volume to 200 μl. To allow access of ions and ATP to membrane vesicles, alamethicin (5 μl) was added to give a final concentration of ~0.1 mg of alamethicin per mg of protein (Xie et al., 1989). An additional 150 μl of ice-cold distilled water was added to each tube. Ouabain, a specific inhibitor of NKA (Wallick and Schwartz, 1988), was placed in half the tubes: 5 μl of a concentrated stock solution was added to bring the final ouabain concentration of 1.25 mM while the remaining tubes received 5 μl of distilled water. The tubes were pre-incubated in the dark at 37 °C for 5 min in a water bath. Then freshly prepared ATP solution was added to each tube (40 μl), making the final ATP concentration 2.0 mM, bringing the reaction mixture volume to 400 μl and the concentration of the NKA buffer down to single strength. After a 30 min ATP hydrolysis period at 37 °C, the reaction was stopped by the addition of 150 ml of 20% ice-cold trichloroacetic acid (TCA) and the tubes were placed on ice for 20 min with occasional shaking.

ATP hydrolysis was determined from the amount of inorganic phosphate released in each reaction tube. To detect inorganic phosphate, each tube was placed in a centrifuge at 3000 rpm (2680×*g*) for 15 min at 4 °C, then 400 μl of the supernatant was removed and mixed with 400 μl of 4.0% FeSO4 solution in ammonium molybdate (1.25*g* of ammonium molybdate in 100 ml of 2.5 N sulfuric acid). Standard solutions containing NaH_2PO_4 equivalent to 0, 10, 62.5, 125, 250 and 500 nmoles of PO_4, were treated similarly. After 5 min at room temperature the tubes with the samples (not the standards) were placed in a centrifuge at 3000 rpm for 10 min to pellet additional precipitates. 250 μl volumes of standards and samples were then placed in separate wells of a 96-well plate and the absorbance was measured at 750 nm in a Perkin Elmer plate reader (Victor V3, Perkin Elmer, CT, USA). NKA activity is calculated as the difference between ATP hydrolysis in the presence and in the absence of ouabain. Values are presented as nmoles ATP hydrolyzed per milligram protein per 30 min.

4.4. Measurement of K^+ efflux

Seven-week-old males were sacrificed by cervical dislocation and 400 μm-thick cortical slice were prepared using a Vibratome. Perfusion for measurement of extracellular potassium (K^+) was performed as previously reported (Deng et al., 2007). Briefly, to measure extracellular K^+, potassium-selective microelectrodes were manufactured by pulling small patch pipettes (~1 μm diameter) and then silanizing the electrode's interior by evaporative deposition of dimethyl-trimethyl-silyamine. After baking the silane to fix it to the glass, the electrode tip was filled with a small volume of the valinomycin-based ionophore cocktail Selectophore 60,525 (Sigma-Aldrich) and backfilled with 100 mM KCl. Microelectrode voltages were measured using a patch-clamp amplifier in current-clamp mode, and digitized and recorded using IgorPro software as we have done in the past for whole-cell recordings (Deng et al., 2007). The K^+-selective microelectrode was placed in layer II/III of slices from the FC. The microelectrodes were calibrated for each experiment using sodium (Na^+) and K^+-containing standard solutions, and in all cases the

microelectrode selectivity for K^+/Na^+ exceeded 20:1. Changes in the K^+ concentration were measured upon addition of the Na^+/K^+ ATPase inhibitor ouabain (100 μM), across genotypes. Analysis was not continued beyond the point at which the average K+ levels exceeded 10 mM, as this was frequently due to a sudden and large jump in K^+ (>20 mM) that is a hallmark of pathological spreading depression (a wave of tissue damage induced by prolonged ouabain application and ischemic insults).

4.5. Golgi staining

Seven-week-old male mice were sacrificed and the brain was rapidly removed and rinsed twice in sterile water. The anterior part of the brain was then blocked by a coronal cut at the level of the optic chiasm and the tissue block was processed following the instructions provided in the FD Rapid GolgiStain kit (FD Neuro Technologies Inc. (www.fdneurotech.com). Briefly, the samples were immersed in a mix of solution solutions A and B at room temperature in the dark for 6 h. The solution was then replaced by a fresh one and the samples were kept in the dark for 10 days. At this time, the samples were transferred to a solution of PBS 1X/30% sucrose for 2 days at 4C, before being placed twice in fresh solution C for 24 h days at 4C. Thereafter, they were frozen on dry ice, embedded in Optimal Cutting Temperature Compound (OCT, Sakura Finetelk, Torrance, CA) and cryostat-sectioned at 100μm intervals, with the cryostat chamber temperature set at −24 °C. The sections were then directly mounted onto 2% gelatin-coated slides, allowed to dry in a slide folder for 2 h in the dark), stained as recommended by the Rapid Golgi Stain manufacturer, and counterstained with 0.1% thionin for 30 sec. After dehydration in ethanol (50, 75, 95, and 100%; 4 min in each bath), the sections were cleared in xylene, and coverslipped.

4.6. Sholl analysis

Pyramidal neurons stained by the Golgi method and located in layers II/III of the frontal cortex were selected for analysis of basal dendritic arborization using the Sholl quantitation method. Sections were imaged on a Zeiss Axioplan microscope (Carl Zeiss Microimaging, Inc., Thornwood, NY) coupled to a Retiga2000R camera (QImaging, Surrey, BC, Canada) and using a Ludl motorized stage (Ludl Electronics Production, Hawthorne, NY). Neurons in Layer II/III presenting an intact dendritic arborization and whose cell bodies were located approximately in the middle of the section (z axis) were analyzed. After optimizing the bright field lighting parameters (Kholer illumination), each neuron was visualized at 40× magnification and each dendrite was traced from its origin on the neuronal cell body (=0 or reference point in z axis) to its end. Completed tracings of dendritic arborization were then visualized using the Neurolucida three-dimensional (3D) neuron reconstruction system and quantified by Sholl analysis using the NeuroExplorer analysis software (version 5.05.1, MicroBrightField, Inc. Williston, VT). Twenty-five neurons per genotype (5 animals/genotype, 5 neurons/animal) were analyzed.

4.7. Statistical analysis

All statistical analyses were performed using SPSS software (SPSS Inc, Chicago, Il), SigmaStat (Systat Software Inc., San Jose, CA) or GraphPad Prism software (GraphPad Software, LaJolla, CA). Genotype differences were analyzed using a one-way ANOVA

(normal distribution, equal variance) followed by the Holm-Sidak post-hoc tests or the Kruskal-Wallis one-way analysis of variance on ranks followed by Dunn's Method pairwise comparison procedure when the normality test failed. In cases that only two genotypes were compared, the results were analyzed using the Student's *t* test. Data are expressed as means ± SEM. $p < 0.05$ was considered significant for all tests.

Acknowledgement

Funding sources.

This work was supported by the Northwest Rett Syndrome Foundation; International Rett Syndrome Association (IRSA20808); NIH grants 8P51-OD-11092-53 for the operation of the Oregon National Primate Research Center (S.R.O.), MH-77647 (J.R), NS064317 (M.F.), EY09532 (N.A.D.) and EY06915 (N.A.D.), International Rett Syndrome Foundation, IRSF (V.M.), and the Collins Medical Trust (V.M.).

Abbreviations:

RTT	Rett Syndrome
MeCP2	methyl-CpG binding protein 2
FXYD1	FXYD (phenyl alanine-any amino acid, tyrosine, aspartic acid domain-containing transport regulator 1
NKA	Sodium/potassium adenosine triphosphatase

References

Ahlers BA, Zhang X-Q, Moorman JR, Rothblum LI, Carl LL, Song J, Wang J, Geddis LM, Tucker AL, Mounsey JP, Cheung JY, 2005 Identification of an endogenous inhibitor of the cardiac Na^+/CA^{2+} exchanger: phospholemman. J. Biol. Chem 280, 19875–19882. [PubMed: 15774479]

Amir RE, Van den Veyver IB, Wan M, Tran CQ, Francke U, Zoghbi HY, 1999 Rett syndrome is caused by mutations in X-linked *MECP2*, encoding methyl-CpG binding protein 2. Nat. Genet 23, 185–188. [PubMed: 10508514]

Armstrong D, Dunn JK, Antalffy B, Trivedi R, 1995 Selective dendritic alterations in the cortex of Rett syndrome. J. Neuropathol. Exp. Neurol 54, 195–201. [PubMed: 7876888]

Armstrong DD, Dunn K, Antalffy B, 1998 Decreased dendritic branching in frontal, motor and limbic cortex in Rett syndrome compared with trisomy 21. J. Neuropathol. Exp. Neurol 57, 1013–1017. [PubMed: 9825937]

Ballas N, Lioy DT, Grunseich C, Mandel G, 2009 Non-cell autonomous influence of MeCP2-deficient glia on neuronal dendritic morphology. Nat. Neurosci 12, 311–317. [PubMed: 19234456]

Banine F, Matagne V, Sherman LS, Ojeda SR, 2011 Brain region-specific expression of Fxyd1, an MeCP2 target gene, is regulated by epigenetic mechanisms. J Neurosci Res. 89, 840–851. [PubMed: 21394759]

Béguin P, Crambert G, Monnet-Tschudi F, Uldry M, Horisberger J-D, Garty H, Geering K, 2002 FXYD7 is a brain-specific regulator of Na, K-ATPase alpha1-beta isozymes. EMBO J. 21, 3264–3273. [PubMed: 12093728]

Belichenko NP, Belichenko PV, Li HH, Mobley WC, Francke U, 2008 Comparative study of brain morphology in Mecp2 mutant mouse models of Rett syndrome. J. Comp Neurol 508, 184–195. [PubMed: 18306326]

Belichenko PV, Dahlstrom A, 1995 Studies on the 3-dimensional architecture of dendritic spines and varicosities in human cortex by confocal laser scanning microscopy and Lucifer yellow microinjections. J. Neurosci. Methods 57, 55–61. [PubMed: 7791365]

Belichenko PV, Hagberg B, Dahlstrom A, 1997 Morphological study of neocortical areas in Rett syndrome. Acta Neuropathol. (Berl) 93, 50–61. [PubMed: 9006657]

Belichenko PV, Wright EE, Belichenko NP, Masliah E, Li HH, Mobley WC, Francke U, 2009 Widespread changes in dendritic and axonal morphology in Mecp2-mutant mouse models of Rett syndrome: evidence for disruption of neuronal networks. J. Comp Neurol 514, 240–258. [PubMed: 19296534]

Bienvenu T, Carrié A, de Roux N, Vinet M-C, Jonveaux P, Cuvert P, Villard L, Arzimanoglou A, Beldjord C, Fontes M, Tardieu M, Chelly J, 2000 *MECP2* mutations account for most cases of typical forms of Rett syndrome. Hum. Mol. Genet 9, 1377–1384. [PubMed: 10814719]

Bienvenu T, Chelly J, 2006 Molecular genetics of Rett syndrome: When DNA methylation goes unrecognized. Nat. Rev. Genet 7, 415–426. [PubMed: 16708070]

Bossuyt J, Despa S, Han F, Hou Z, Robia SL, Lingrel JB, Bers DM, 2009 Isoform specificity of the Na/K-ATPase association and regulation by phospholemman. J. Biol. Chem 284, 26749–26757. [PubMed: 19638348]

Chahrour M, Zoghbi HY, 2007 The story of Rett syndrome: from clinic to neurobiology. Neuron 56, 422–437. [PubMed: 17988628]

Chang JT, Lowery LA, Sive H, 2012 Multiple roles for the Na, K-ATPase subunits, Atp1a1 and Fxyd1, during brain ventricle development. Dev. Biol 368, 312–322. [PubMed: 22683378]

Chang Q, Khare G, Dani V, Nelson S, Jaenisch R, 2006 The disease progression of Mecp2 mutant mice is affected by the level of BDNF expression. Neuron 49, 341–348. [PubMed: 16446138]

Chao HT, Zoghbi HY, 2012 MeCP2: only 100% will do. Nat. Neurosci 15, 176–177. [PubMed: 22281712]

Chen RZ, Akbarian S, Tudor M, Jaenisch R, 2001 Deficiency of methyl-CpG binding protein-2 in CNS neurons results in a Rett-like phenotype in mice. Nat. Genet 327, 331.

Crambert G, Füzesi M, Garty H, Karlish S, Geering K, 2002 Phospholemman (FXYD1) associates with Na, K-ATPase and regulates its transport properties. Proc. Natl. Acad. Sci. USA 99, 11476–11481. [PubMed: 12169672]

Crambert G, Geering K, 2003 FXYD proteins: new tissue-specific regulators of the ubiquitous Na,K-ATPase. Sci. STKE 2003:RE1. [PubMed: 12538882]

Deng V, Matagne V, Banine F, Frerking M, Ohliger P, Budden S, Pevsner J, Dissen GA, Sherman LS, Ojeda SR, 2007 FXYD1 is an MeCP2 target gene overexpressed in the brains of Rett syndrome patients and Mecp2-null mice. Hum. Mol. Genet 16, 640–650. [PubMed: 17309881]

Desfrere L, Karlsson M, Hiyoshi H, Malmersjo S, Nanou E, Estrada M, Miyakawa A, Lagercrantz H, El MA, Lal M, Uhlen P, 2009 Na, K-ATPase signal transduction triggers CREB activation and dendritic growth. Proc. Natl. Acad. Sci. USA 106, 2212–2217. [PubMed: 19164762]

Feschenko MS, Donnet C, Wetzel RK, Asinovski NK, Jones LR, Sweadner KJ, 2003 Phospholemman, a single-span membrane protein, is an accessory protein of Na, K-ATPase in cerebellum and choroid plexus. J. Neurosci 23, 2161–2169. [PubMed: 12657675]

Fukuda T, Itoh M, Ichikawa T, Washiyama K, Goto Y, 2005 Delayed maturation of neuronal architecture and synaptogenesis in cerebral cortex of Mecp2-deficient mice. J. Neuropathol. Exp. Neurol 64, 537–544. [PubMed: 15977646]

Garcia-Rudaz C, Deng V, Matagne V, Ronnekleiv O, Bosch M, Han V, Percy AK, Ojeda SR, 2008 FXYD1, a modulator of Na(+), K(+)-ATPase activity, facilitates female sexual development by maintaining GnRH neuronal excitability. J. Neuroendocrinol 21, 108–122.

Glanzman DL, 2010 Ion pumps get more glamorous. Nat. Neurosci 13, 4–5. [PubMed: 20033078]

Guy J, Gan J, Selfridge J, Cobb S, Bird A, 2007 Reversal of neurological defects in a mouse model of Rett syndrome. Science 315, 1143–1147. [PubMed: 17289941]

Guy J, Hendrich B, Holmes M, Martin JE, Bird A, 2001 A mouse *Mecp2*-null mutation causes neurological symptoms that mimic Rett syndrome. Nat. Genet 27, 322–326. [PubMed: 11242117]

Jia LG, Donnet C, Bogaev RC, Blatt RJ, McKinney CE, Day KH, Berr SS, Jones LR, Moorman JR, Sweadner KJ, Tucker AL, 2005 Hypertrophy, increased ejection fraction, and reduced Na, K-ATPase activity in phospholemman-deficient mice. Am. J. Physiol. Heart Circ. Physiol 288, H1982–H1988. [PubMed: 15563542]

Jordan C, Li HH, Kwan HC, Francke U, 2007 Cerebellar gene expression profiles of mouse models for Rett syndrome reveal novel MeCP2 targets. BMC. Med. Genet 8, 36. [PubMed: 17584923]

Kishi N, Macklis JD, 2004 MECP2 is progressively expressed in post-migratory neurons and is involved in neuronal maturation rather than cell fate decisions. Mol. Cell Neurosci 27, 306–321. [PubMed: 15519245]

Kishi N, Macklis JD, 2005 Dissecting MECP2 function in the central nervous system. J. Child Neurol 20, 753–759. [PubMed: 16225831]

Lees GJ, 1991 Inhibition of sodium-potassium-ATPase: a potentially ubiquitous mechanism contributing to central nervous system neuropathology. Brain Res. Brain Res. Rev 16, 283–300. [PubMed: 1665097]

Matagne V, Budden S, Ojeda SR, Raber J, 2013 Correcting deregulated Fxyd1 expression ameliorates a behavioral impairment in a mouse model of Rett syndrome. Brain Res. 1496, 104–114. [PubMed: 23246925]

Miralves J, Magdeleine E, Joly E, 2007 Design of an improved set of oligonucleotide primers for genotyping MeCP2tm1.1Bird KO mice by PCR. Mol. Neurodegener 2, 16. [PubMed: 17764542]

Mirza MA, Zhang XQ, Ahlers BA, Qureshi A, Carl LL, Song J, Tucker AL, Mounsey JP, Moorman JR, Rothblum LI, Zhang TS, Cheung JY, 2004 Effects of phospholemman downregulation on contractility and [Ca(2+)]i transients in adult rat cardiac myocytes. Am. J. Physiol Heart Circ. Physiol 286, H1322–H1330. [PubMed: 14684371]

Mounsey JP, John JEI, Helmke SM, Such EW, Gilbert J, Roses AD, Perrymann MB, Jones LR, Moorman JR, 2000 Phospholemman is a substrate for myotonic dystrophy protein kinase. J. Biol. Chem 275, 23362–23367. [PubMed: 10811636]

Mounsey JP, Lu KP, Patel MK, Chen ZH, Horne LT, John III JE, Means AR, Jones LR, Moorman JR, 1999 Modulation of Xenopus oocyte-expressed phospholemman-induced ion currents by co-expression of protein kinases. Biochim. Biophys. Acta 1451, 305–318. [PubMed: 10556585]

Mullaney BC, Johnston MV, Blue ME, 2004 Developmental expression of methyl-CpG binding protein 2 is dynamically regulated in the rodent brain. Neuroscience 123, 939–949. [PubMed: 14751287]

Palmer CJ, Scott BT, Jones LR, 1991 Purification and complete sequence determination of the major plasma membrane substrate for cAMP-dependent protein kinase and protein kinase C in myocardium. J. Biol. Chem 266, 11126–11130. [PubMed: 1710217]

Presti DF, Jones LR, Lindemann JP, 1985 Isoproterenol-induced phosphorylation of a 15-kilodalton sarcolemmal protein in intact myocardium. J. Biol. Chem 260, 3860–3867. [PubMed: 2982878]

Pulver SR, Griffith LC, 2010 Spike integration and cellular memory in a rhythmic network from Na +/K+ pump current dynamics. Nat. Neurosci 13, 53–59. [PubMed: 19966842]

Robinson L, Guy J, McKay L, Brockett E, Spike RC, Selfridge J, De SD, Merusi C, Riedel G, Bird A, Cobb SR, 2012 Morphological and functional reversal of phenotypes in a mouse model of Rett syndrome. Brain:[Epub ahead of print].

Shahbazian MD, Antalffy B, Armstrong DL, Zoghbi HY, 2002a Insight into Rett syndrome: MeCP2 levels display tissue- and cell-specific differences and correlate with neuronal maturation. Hum. Mol. Genet 11, 115–124. [PubMed: 11809720]

Shahbazian MD, Young JI, Yuva-Paylor LA, Spencer CM, Antalffy BA, Noebels JL, Armstrong DL, Paylor R, Zoghbi HY, 2002b Mice with truncated MeCP2 recapitulate many Rett syndrome features and display hyperacetylation of histone H3. Neuron 35, 243–254. [PubMed: 12160743]

Shahidullah M, Mandal A, Beimgraben C, Delamere NA, 2012 Hyposmotic stress causes ATP release and stimulates Na, K-ATPase activity in porcine lens. J. Cell Physiol 227, 1428–1437. [PubMed: 21618533]

Shiina N, Yamaguchi K, Tokunaga M, 2010 RNG105 deficiency impairs the dendritic localization of mRNAs for Na+/K+ ATPase subunit isoforms and leads to the degeneration of neuronal networks. J. Neurosci 30, 12816–12830. [PubMed: 20861386]

Skene PJ, Illingworth RS, Webb S, Kerr AR, James KD, Turner DJ, Andrews R, Bird AP, 2010 Neuronal MeCP2 is expressed at near histone-octamer levels and globally alters the chromatin state. Mol. Cell 37, 457–468. [PubMed: 20188665]

Smith PK, Krohn RI, Hermanson GT, Mallia AK, Gartner FH, Provenzano MD, Fujimoto EK, Goeke NM, Olson BJ, Klenk DC, 1985 Measurement of protein using bicinchoninic acid. Anal. Biochem 150, 76–85. [PubMed: 3843705]

Tamiya S, Okafor MC, Delamere NA, 2007 Purinergic agonists stimulate lens Na-K-ATPase-mediated transport via a Src tyrosine kinase-dependent pathway. Am. J. Physiol Cell Physiol 293, C790–C796. [PubMed: 17522142]

Tropea D, Giacometti E, Wilson NR, Beard C, McCurry C, Fu DD, Flannery R, Jaenisch R, Sur M, 2009 Partial reversal of Rett Syndrome-like symptoms in MeCP2 mutant mice. Proc. Natl. Acad. Sci. USA 106, 2029–2034. [PubMed: 19208815]

Tudor M, Akbarian S, Chen RZ, Jaenisch R, 2002 Transcriptional profiling of a mouse model for Rett syndrome reveals subtle transcriptional changes in the brain. Proc. Natl. Acad. Sci. USA 99, 15536–15541. [PubMed: 12432090]

Walaas SI, Czernik AJ, Olstad OK, Sletten K, Walaas O, 1994 Protein kinase C and cyclic AMP-dependent protein kinase phosphorylate phospholemman, an insulin and adrenalin-regulated membrane phosphoprotein, at specific sites in the carboxy terminal domain. Biochem. J 304, 635–640. [PubMed: 7999001]

Walaas SI, Horn RS, Albert KA, Adler A, Walaas O, 1988 Phosphorylation of multiple sites in a 15,000 dalton proteolipid from rat skeletal muscle sarcolemma, catalyzed by adenosine 3′,5′-monophosphate-dependent and calcium/phospholipid-dependent protein kinases. Biochim. Biophys. Acta 968, 127–137. [PubMed: 3337842]

Wallick ET, Schwartz A, 1988 Interaction of cardiac glycosides with Na+, K+-ATPase. Methods Enzymol. 156, 201–213. [PubMed: 2835605]

Wan M, Lee SS, Zhang X, Houwink-Manville I, Song HR, Amir RE, Budden S, Naidu S, Pereira JL, Lo IF, Zoghbi HY, Schanen NC, Francke U, 1999 Rett syndrome and beyond: recurrent spontaneous and familial MECP2 mutations at CpG hotspots. Am. J. Hum. Genet 65, 1520–1529. [PubMed: 10577905]

Wang F, Smith NA, Xu Q, Fujita T, Baba A, Matsuda T, Takano T, Bekar L, Nedergaard M, 2012 Astrocytes modulate neural network activity by Ca(2)(+)-dependent uptake of extracellular K(+). Sci. Signal 5:ra26. [PubMed: 22472648]

Xie Z, Askari A, 2002 Na(+)/K(+)-ATPase as a signal transducer. Eur. J. Biochem 269, 2434–2439. [PubMed: 12027880]

Xie ZJ, Wang YH, Ganjeizadeh M, McGee R Jr., Askari A, 1989 Determination of total (Na+ + K+)-ATPase activity of isolated or cultured cells. Anal. Biochem 183, 215–219. [PubMed: 2560348]

Zhang XQ, Moorman JR, Ahlers BA, Carl LL, Lake DE, Song J, Mounsey JP, Tucker AL, Chan YM, Rothblum LI, Stahl RC, Carey DJ, Cheung JY, 2006 Phospholemman overexpression inhibits Na+-K+-ATPase in adult rat cardiac myocytes: relevance to decreased Na+ pump activity in postinfarction myocytes. J. Appl. Physiol 100, 212–220. [PubMed: 16195392]

Zhang XQ, Qureshi A, Song J, Carl LL, Tian Q, Stahl RC, Carey DJ, Rothblum LI, Cheung JY, 2003 Phospholemman modulates Na+/Ca2+ exchange in adult rat cardiac myocytes. Am. J. Physiol Heart Circ. Physiol 284, H225–H233. [PubMed: 12388273]

Zhang Y, Chen M, Qiu Z, Hu K, McGee W, Chen X, Liu J, Zhu L, Wu JY, 2016 MiR-130a regulates neurite outgrowth and dendritic spine density by targeting MeCP2. Protein Cell 7, 489–500. [PubMed: 27245166]

Zhou Z, Hong EJ, Cohen S, Zhao WN, Ho HY, Schmidt L, Chen WG, Lin Y, Savner E, Griffith EC, Hu L, Steen JA, Weitz CJ, Greenberg ME, 2006 Brain-Specific Phosphorylation of MeCP2 Regulates Activity-Dependent Bdnf Transcription, Dendritic Growth, and Spine Maturation. Neuron 52, 255–269. [PubMed: 17046689]

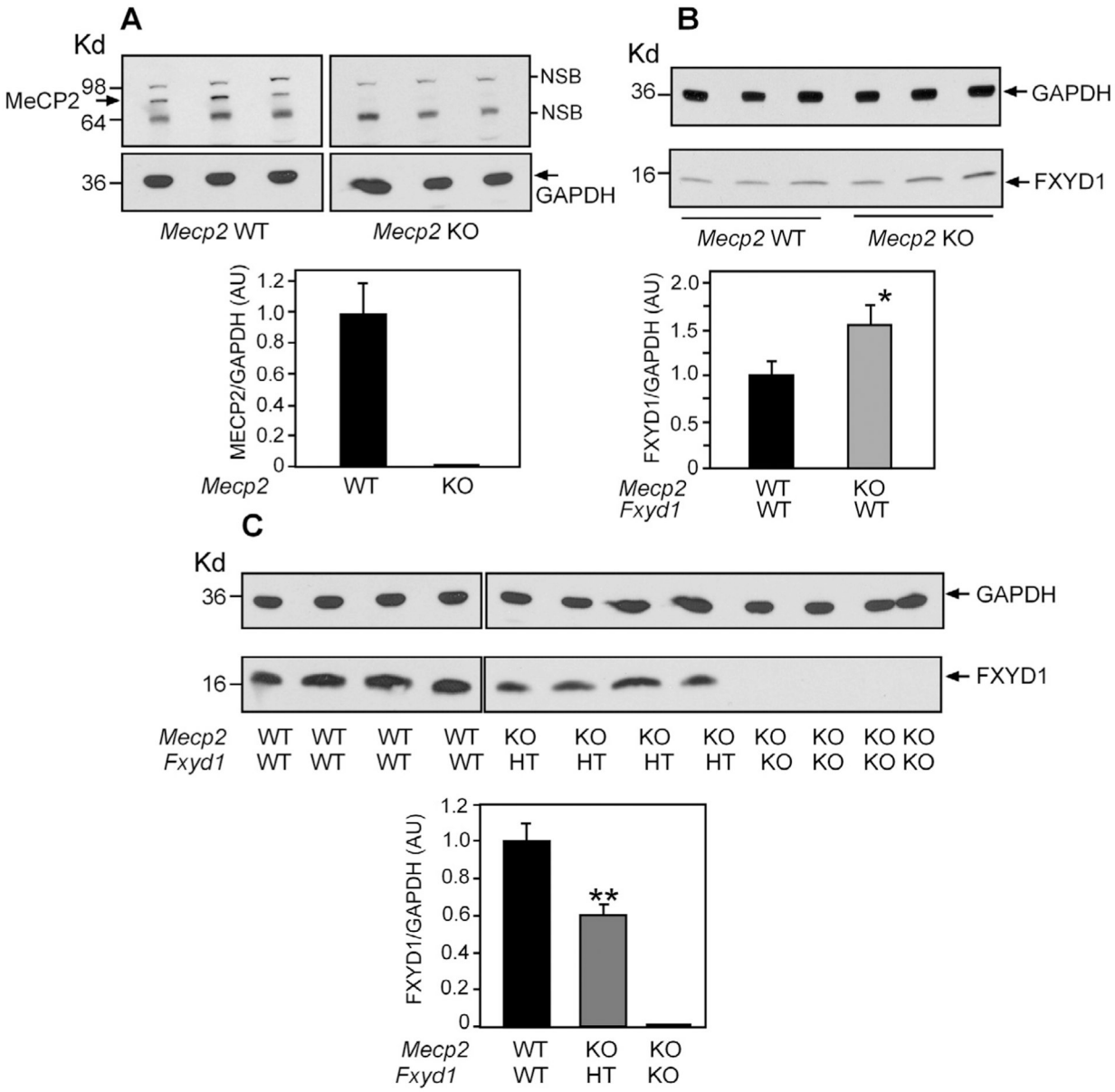

Fig. 1.

Changes in the content of Fxyd1 and MeCP2 in the FC of male mice lacking *Mecp2* and either one or two *Fxyd1* alleles as assessed by Western blotting. A, *Upper panels:* The top blots show that MeCP2 is detected in the FC of 7-week -old *Mecp2* WT animals, but not in *Mecp2* KO mice (n = 3 animals per group). The bottom blots depicts the GAPDH content (used as a loading control) detected in each sample. NSB = non-specific bands present in all samples regardless of *Mecp2* genotype. *Lower panel:* Densitometric analysis of the changes in MeCP2 content seen in the upper panels. Values represent the ratio between Fxyd1 and GAPDH and are expressed as arbitrary units. B, *Upper panels:* The bottom blot shows that the content of Fxyd1 increases in the FC of *Mecp2* KO male mice (n = 3 animals per group). The membrane was exposed to film for a short time to more clearly visualize the increase in Fxyd1 levels. The blot on top depicts the GAPDH content detected in each sample. *Lower*

panel: densitometric analysis of the changes in Fxyd1 content seen in the upper panels. C, *Upper panels:* The bottom blots shows that the Fxyd1 content decreases by about 50% in the FC of mice lacking one *Fxyd1* allele and is undetectable in *Fxyd1* null mice (n = 4 animals per group). The membranes were exposed longer than in panel B to be certain that Fxyd1 was absent in the FC of *Fxyd1* KO mice. The blots on top depict the GAPDH content of each sample. *Lower panel:* Densitometric analysis of the changes in Fxyd1 content shown in the upper panels. Each lane was loaded with 25 μg of proteins extracted from the FC of a single mouse. WT/WT = WT for both *Mecp2* and *Fxyd1; KO*/WT = *Mecp2* KO/*Fxyd1* WT; *KO*/HT = *Mecp2* KO lacking one *Fxyd1* allele; *KO/KO* = *Mecp2* KO lacking both *Fxyd1* alleles. Vertical bars are mean ± SEM and numbers on top of bars are number of animals/group. * = $p < 0.05$ and ** = $p < 0.01$ vs. WT controls.

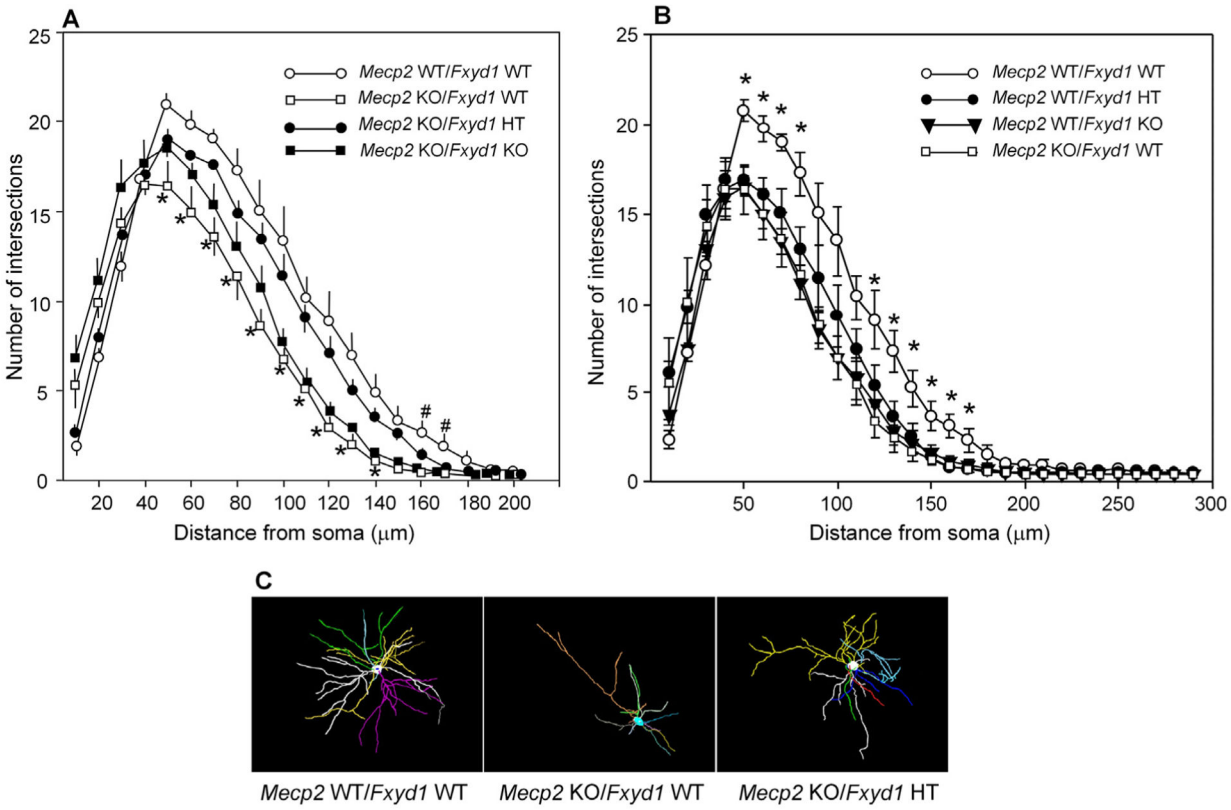

Fig. 2.

Deletion of one *Fxyd1* allele rescues the deficits in neuronal dendritic arborization observed in *Mecp2* KO mice: **A,** Sholl analysis showing that *Mecp2* null neurons of the FC have a significantly lower number and length of dendrites than WT neurons, and that the WT phenotype is rescued by deletion of one *Fxyd1* allele. Values are mean ± SEM., * = $p < 0.05$ vs. either *Mecp2* KO/*Fxyd1* HT or *Mecp2* WT/*Fxyd1* WT group; # = $p < 0.05$ vs. all other groups (one-way ANOVA followed by the Student-Newman-Keuls *post-hoc* test). B, Sholl analysis showing that deleting one or two *Fxyd1* alleles impairs dendritic arborization in neurons with an intact *Mecp2* gene, resulting in a phenotype similar to that seen in *Mecp2 KO* neurons. The neurite profile of *Mecp2* WT/*Fxyd1* WT and *Mecp2* KO/*Fxyd1* WT neurons shown in A is re-depicted in B for comparative purposes. * = $p < 0.05$ vs. all other groups (one-way ANOVA followed by the Student-Newman-Keuls *post-hoc* test). Each group represents the mean of 25 neurons derived from 5 different 7-week-old animals. **C,** Examples of 3-D reconstructions of neuronal phenotypes shown in A.

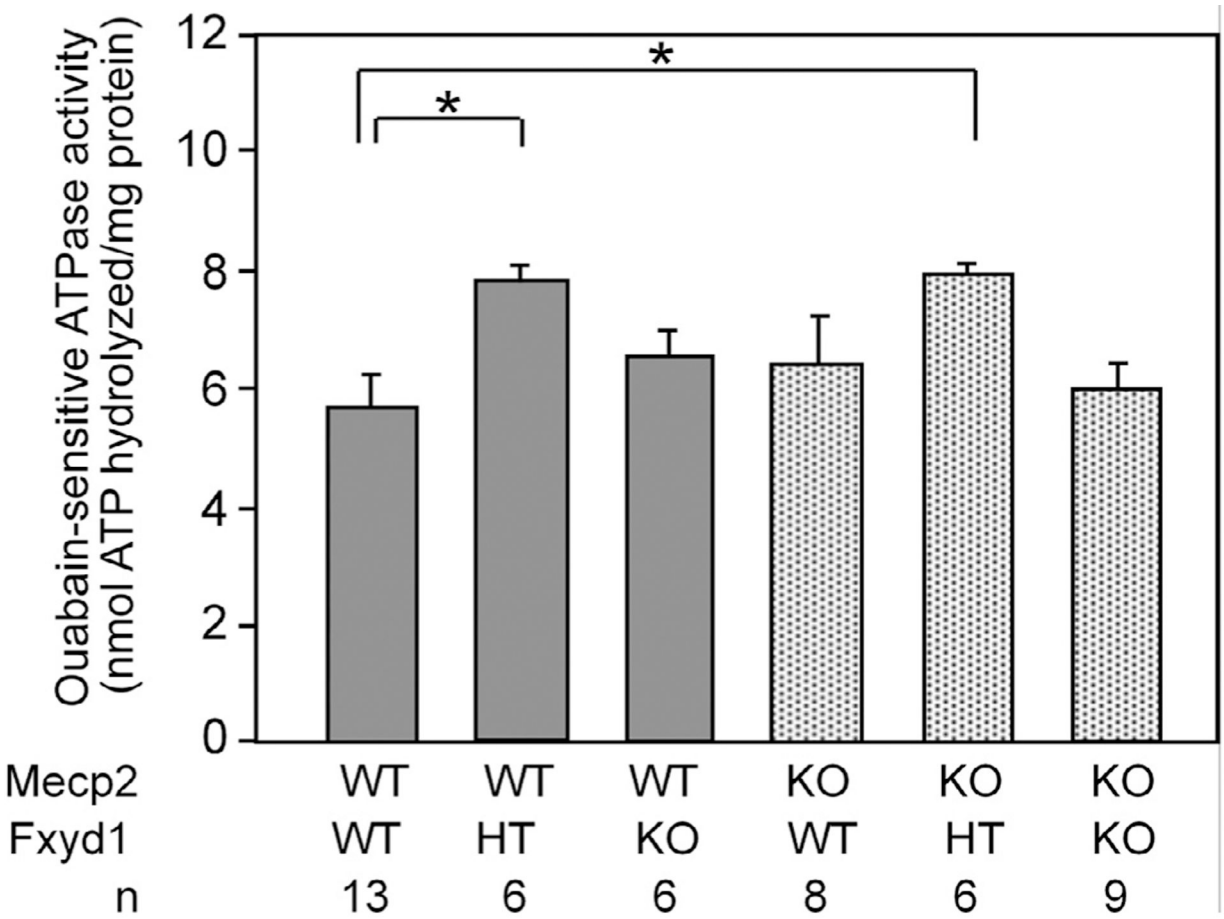

Fig. 3.

NKA enzymatic activity is increased in the FC of mice lacking one *Fxyd1* allele. Ouabain-sensitive NKA activity was measured in the FC using a biochemical assay that measures ATP hydrolysis in the presence of ouabain (1.25 mM). NKA activity was normalized to the total amount of protein (mg) as measured by the bicinchoninic acid assay. * = $P < 0.05$, Kruskal-Wallis test with Dunn's multiple comparison vs the WT group. Bars are mean ± SEM. Number of animals/genotype are shown for each genotype (n).

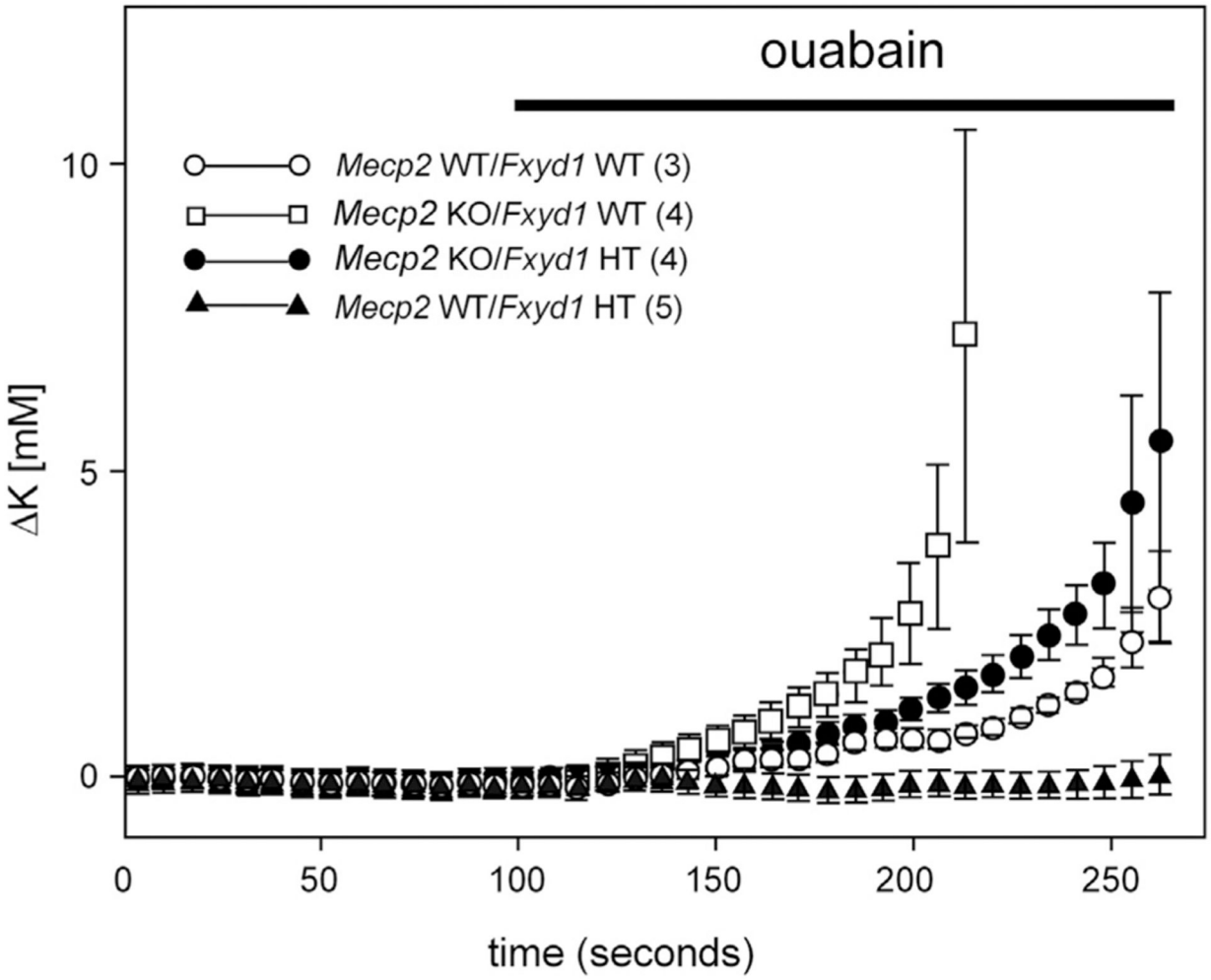

Fig. 4.

Ouabain-induced accumulation of extracellular K^+ is enhanced in *Mecp2* KO mice, and this enhancement is reversed by deletion of one *Fxyd1* allele. Changes in the extracellular K^+ levels upon ouabain addition (100 μM) were assessed using K^+-selective microelectrodes placed in layer II/III of the FC. In all cases, the selectivity of electrodes for K^+ relative to Na^+ was a minimum of 30:1, and electrode selectivity and accuracy was confirmed by calibration in every experiment. At rest, the slice was perfused with ACSF containing 2.5 mM K^+. Addition of ouabain to the incubation medium (horizontal bar) blocked NKA activity and increased the extracellular K^+ levels, a change that occurred more rapidly and more pronouncedly in *Mecp2*-null mice. Deletion of one *Fxyd1* allele restored a WT response in *Mecp2* null mice. K^+ levels were examined until they reache ~10 mM above basal levels, as larger increases than this were generally associated with regenerative seizure activity and cell swelling throughout the tissue, as is commonly observed in response to prolonged application of ouabain. The numbers in parenthesis correspond to the number of cells recorded per genotype, using 2–5 animals per group. The values shown are changes in extracellular K+ levels/neuron (mean ± SEM).